Draft version July 15, 2008
Preprint typeset using LaTeX style emulateapj v. 04/21/05

THE CLUSTERING OF SDSS GALAXY GROUPS: MASS AND COLOR DEPENDENCE

Yu Wang[1,2,6], Xiaohu Yang[2,6], H.J. Mo[3], Frank C. van den Bosch[4], Simone M. Weinmann[5], Yaoquan Chu[1]

Draft version July 15, 2008

ABSTRACT

We use a large sample of galaxy groups selected from the SDSS data release 4 with an adaptive halo-based group finder to probe how the clustering strength of groups depends on their masses and colors. In particular, we determine the relative biases of groups of different masses, as well as that of groups with the same mass but with different colors (either that of the central galaxy, or the total color of all group members). In agreement with previous studies, we find that more massive groups are more strongly clustered, and the inferred mass dependence of the halo bias is in good agreement with predictions for the ΛCDM concordance cosmology. Regarding the color dependence, we find that groups with red centrals are more strongly clustered than groups of the same mass but with blue centrals. Similar results are obtained when the color of a group is defined to be the total color of its member galaxies. The color dependence is more prominent in less massive groups and becomes insignificant in groups with masses $\gtrsim 10^{14}\,h^{-1}\mathrm{M}_{\odot}$. These results are consistent with those obtained by Yang et al. from an analysis of the 2dFGRS, but inconsistent with those obtained by Berlind et al. , who also used an SDSS group catalogue. We construct a mock galaxy redshift survey from the large Millennium N-body simulation that is populated with galaxies according to the semi-analytical model of Croton et al. Applying our group finder to this mock survey, and analyzing the mock data in exactly the same way as the true data, we are able to accurately recover the intrinsic mass and color dependencies of the halo bias in the model. Interestingly, the semi-analytical model reveals the same color dependence of the halo bias as we find in our group catalogue. In halos with $M \sim 10^{12}\,h^{-1}\mathrm{M}_{\odot}$, though, the strength of the color dependence is much stronger in the model than in the data. We discuss these results in light of the assembly bias of dark matter halos and the star formation histories of galaxies.

Subject headings: dark matter - large-scale structure of the universe - galaxies: halos

1. INTRODUCTION

In the standard cold dark matter (CDM) paradigm of structure formation, virialized CDM halos are considered to be the building blocks of the mass distribution in the Universe. The properties of dark matter halos, as well as their formation histories and clustering properties, have been studied in great detail using both numerical simulations and analytical approaches such as the (extended) Press Schechter (1974) formalism. These studies have shown that halo bias is mass dependent, in that more massive halos are more strongly clustered (e.g., Mo & White 1996; Sheth & Tormen 1999; Sheth, Mo & Tormen 2001; Seljak & Warren 2004; Tinker et al. 2005). This mass dependence of the halo bias has played a crucial role in our understanding of the correlation function of both dark matter and galaxies, via the halo model (e.g., Cooray & Sheth 2002), the halo occupation model (e.g., Jing, Mo & Börner 1998; Seljak 2000; Peacock & Smith 2000; Berlind & Weinberg 2002; Magliocchetti & Porciani 2003; Berlind et al. 2003; Zheng et al. 2005), and the conditional luminosity function (CLF) model (e.g., Yang, Mo & van den Bosch 2003; van den Bosch, Yang & Mo 2003; Vale & Ostriker 2006; Cooray 2006; van den Bosch et al. 2007).

Observationally, the clustering strength of galaxy systems (groups and clusters) is found to increase with their mean separation $d \equiv n^{-1/3}$, with n the number density of objects (e.g. Bahcall & West 1992; Zandivarez et al. 2003; Padilla et al. 2004; Yang et al. 2005b). Assuming that richer groups are statistically associated with more massive halos, one can estimate the halo masses of galaxy groups using a theoretical halo mass function, such as the one given by the current ΛCDM model (see Yang et al. 2005b; Berlind et al. 2006a; Yang et al. 2007). Thus the relation between mean separation and clustering strength can be converted into a relation between halo mass and halo bias. As shown in Yang et al. (2005b), the mass dependence of the halo bias obtained this way from galaxy groups is in good agreement with the prediction of the current ΛCDM model.

In addition to the mass dependence, recent simulations have shown that halo bias also depends on the assembly history. Using N-body simulations, Sheth & Tormen (2004) studied the environmental dependence of halo assembly and found that dark matter halos in dense environments assemble at slightly earlier times than halos of the same mass in low density regions. Gao et al. (2005) used a very large, high-resolution numerical simulation of structure formation in a ΛCDM cosmology to reexamine the mass and age dependence of halo bias. They found

[1] Center for Astrophysics, University of Science and Technology of China, 230026, P. R. China
[2] Shanghai Astronomical Observatory, the Partner Group of MPA, Nandan Road 80, Shanghai 200030, China
[3] Department of Astronomy, University of Massachusetts, Amherst MA 01003-9305
[4] Max-Planck Institute for Astronomy, D-69117 Heidelberg, Germany
[5] Max-Planck-Institut für Astrophysik, Karl-Schwarzschild-Strasse 1, 85748 Garching, Germany
[6] Joint Institute for Galaxy and Cosmology (JOINGC) of Shanghai Astronomical Observatory and University of Science and Technology of China

that, for halos of $M \leq 10^{13}\,h^{-1}\mathrm{M}_{\odot}$ at redshift $z = 0$, the bias factor depends not only on halo mass but also on the halo assembly time. This result has been confirmed by a number of subsequent investigations (Harker et al. 2006; Wechsler et al. 2006; Wetzel et al. 2006; Gao & White 2007; Jing, Suto & Mo 2007). The origin of this assembly bias has recently been investigated in a number of papers (Wang, Mo & Jing 2007; Keselman & Nusser 2007; Hahn et al. 2007).

If the properties of galaxies that reside in haloes of a given mass correlate with the assembly history of that halo, the assembly bias will impact the galaxy bias, $b_{\rm gal}$, to the extent that $b_{\rm gal}$ not only depends on halo mass, as generally assumed in HOD and CLF modeling, but also on the formation history of that halo. Using a very crude method for assigning galaxy luminosities to dark matter haloes, Reed et al. (2007) conclude, however, that the luminosity-weighted galaxy ages cannot closely trace the assembly epoch of their dark matter hosts, otherwise the observed color-dependence of the clustering can not be reproduced. Using a galaxy formation model grafted on to the Millennium Simulation, Croton, Gao & White (2007) compared the original simulation to 'shuffled' versions in which the galaxy populations are randomly swapped among haloes of similar mass. They found that the shuffled versions have correlation functions that are different from the original ones at the 5 to 10 percent level, indicating that galaxy properties are (weakly) correlated with the halo assembly history. Unfortunately, since their semi-analytical model is not a perfect representation of the true universe (see e.g., Weinmann et al. 2006b and Baldry et al. 2006), it is unclear whether such a correlation also exists in reality.

To test this, various authors have examined whether there is any sign of assembly bias in the large scale structure of the observed galaxy distribution. Using a galaxy group catalogue constructed from the 2-degree Field Galaxy Redshift Survey (2dFGRS; Colless et al. 2001), Yang et al. (2006) examined how the clustering strength of galaxy groups depends on the star formation activity of the central galaxies. At fixed mass they found that the bias of galaxy groups decreases as the SFR of the central galaxy increases. Assuming that galaxies with a more active SFR are bluer, this implies that groups with a red central are more strongly clustered than groups of the same mass but with a blue central. Surprisingly, a completely opposite trend was found by Berlind et al. (2006a) using the group catalogue constructed by Berlind et al. (2006b) from the Sloan Digital Sky Survey (SDSS; York et al. 2000). They found that massive groups with bluer centrals are *more* strongly biased on large scales than groups of the same mass but with redder centrals. Tinker et al. (2007) used the (projected) galaxy correlation function and galaxy void statistics to test whether the galaxy content of halos of fixed mass is systematically different in low density environments. Using data from the SDSS combined with HOD models, they find that the luminosity and color of field galaxies are determined predominantly by the mass of the halo in which they reside and have little direct dependence on the environment in which the host halo formed. Since, as shown by Sheth & Tormen (2004), the assembly history of a halo is correlated with its environment, this therefore implies that there is no significant correlation between the color of a galaxy and the assembly history of its dark matter halo. Finally, Blanton & Berlind (2006)compared the actual relationship between galaxy colors and large scale density field to that predicted by the null hypothesis that galaxy colors are only dependent on the mass of the halo in which they reside. To this extent, they use a similar shuffling technique as Croton et al. (2007), but using galaxy groups in the SDSS rather than dark matter halos in a semi-analytical model for galaxy formation. They find that shuffled and unshuffled color-density relations agree to better than 5 percent, indicating that the large scale environment of a group has only a very mild impact on the properties of its member galaxies. Clearly, the current status as to whether galaxy properties are correlated with the halo assembly history is still very confusing.

In this paper, we re-examine the dependence of the halo bias on group mass and on the colors of member galaxies, using the galaxy group catalogue recently constructed by Yang et al. (2007) from the SDSS DR4 (Adelman-McCarthy et al. 2006). An important improvement of this catalogue over that of Yang et al. (2006) and Weinmann et al. (2006a) is that group masses are estimated both from the total luminosity and the total stellar mass of member galaxies, allowing us to examine how the results may be affected by the uncertainties in the estimate of group masses. Furthermore, in order to test the impact of the uncertainties in the group finder and in the methods used to assign masses to our groups, we use a mock galaxy redshift survey (hereafter MGRS) constructed from the Millennium semi-analytical galaxy sample (hereafter SAM) of Croton et al. (2006) to test how accurately we can recover the true trends in the semi-analytical model.

This paper is organized as follows. Section 2 describes the galaxy sample and group catalogue used for our analysis, while Section 3 presents our method for estimating the group-galaxy cross-correlation function. Our observational results for the dependence of the group-galaxy cross-correlation on group mass and on the color of the central galaxy are presented in Section 4. The same results. but for the semi-analytical MGRS are presented in Section 5. Finally, in Section 6, we summarize and discuss our findings. Throughout this paper, we adopt the ΛCDM 'concordance' cosmology with $\Omega_m = 0.24$, $\Omega_\Lambda = 0.76$, $h = 0.73$ and $\sigma_8 = 0.77$. Distances are quoted in units of h^{-1}Mpc.

2. GALAXY AND GROUP SAMPLES USED

2.1. *The Observational Samples of Galaxies*

We use galaxy samples constructed from the New York University Value-Added Galaxy Catalogue (NYU-VAGC, see Blanton et al. 2005b). The version of the catalogue used here is based on the SDSS Data Release 4 (Adelman-McCarthy et al. 2006). Only galaxies with redshifts $0.01 \leq z \leq 0.2$, extinction-corrected Petrosian magnitudes $14.5 < r < 17.6$, and redshift completeness $\mathcal{C} > 0.7$ are selected. The r-band and g-band absolute magnitudes are corrected to $z = 0.1$ using the K-correction code of Blanton et al. (2003a) and the luminosity-evolution model of Blanton et al. (2003b). In the apparent-magnitude limits adopted here, the bright end is chosen to avoid the incompleteness due to the large

TABLE 1
Volume-limited Samples of Galaxies

Sample	z	$^{0.1}\mathrm{M}_r - 5\log h$	N_{galaxy} (obs.)	N_{galaxy} (mock)
V1	(0.064, 0.127)	(-22.0, -20.5]	54116	66484
V2	(0.064, 0.157)	(-22.0, -21.0]	39101	51627

Note. — Column 1 indicates the volume-limited galaxy sample ID. Column 2 gives the redshift range of each sample. Column 3 is the absolute-magnitude range. Columns 4 and 5 list the galaxy number in each sample for observational and mock SDSS catalogues, respectively.

TABLE 2
Galaxy Groups in the Observation

ID	$\log M_\mathrm{h}$	z	N_{group} (M_L/M_S)	C0 (M_L/M_S)			C1 (M_L/M_S)	
				Red	Green	Blue	Red	Blue
(1)	(2)	(3)	(4)	(5)	(6)	(7)	(8)	(9)
G1	(12.0, 12.5]	(0.064,0.127)	43233/41314	0.99/0.99	0.87/0.88	0.60/0.66	0.94/0.96	0.65/0.77
G2	(12.5, 13.0]	(0.064,0.127)	15614/15450	1.01/1.01	0.91/0.92	0.67/0.72	0.96/0.99	0.73/0.84
G3	(13.0, 13.5]	(0.064,0.157)	9909/10104	1.03/1.03	0.94/0.95	0.71/0.75	0.99/1.01	0.80/0.88
G4	(13.5, 14.0]	(0.064,0.157)	2976/2826	1.04/1.04	0.96/0.97	0.73/0.75	0.99/1.01	0.86/0.89

Note. — Column 1 indicates the group sample ID. Column 2 indicates the mass range of each group sample in terms of $\log[M_h/\ h^{-1}\mathrm{M}_\odot]$. Column 3 gives the redshift range of each sample. Column 4 lists the group number in the corresponding redshift and mass ranges, where M_L and M_S mean group masses estimated from the ranking of group luminosity $L_{19.5}$ and stellar mass $M_{\rm stellar}$, respectively (Yang et al. 2007). Columns 5-7 list the means of the central galaxy colors (C0) for groups with red, green (galaxies between red and blue Gaussian peaks), blue central galaxies, respectively. Columns 8 and 9 list the means of the total group colors (C1) for groups which are separated into red and blue subsamples in similar numbers. See the text for more details.

TABLE 3
Galaxy Groups in the MGRS

ID	$\log M_\mathrm{h}$	z	N_{group} (M_L/M_S)	C0 (M_L/M_S)			C1 (M_L/M_S)	
				Red	Green	Blue	Red	Blue
(1)	(2)	(3)	(4)	(5)	(6)	(7)	(8)	(9)
S1	(12.0, 12.5]	(0.064,0.127)	46274/44761	0.98/0.99	0.86/0.86	0.53/0.58	0.89/0.90	0.54/0.61
S2	(12.5, 13.0]	(0.064,0.127)	16929/16538	0.98/0.98	0.87/0.89	0.57/0.61	0.90/0.93	0.59/0.68
S3	(13.0, 13.5]	(0.064,0.157)	11139/11231	0.97/0.97	0.89/0.91	0.55/0.60	0.92/0.94	0.61/0.69
S4	(13.5, 14.0]	(0.064,0.157)	3311/3453	0.97/0.97	0.92/0.93	0.47/0.63	0.93/0.94	0.53/0.68

Note. — Similar to Table 2, but for galaxy groups in the semi-analytical Mock Galaxy Redshift Survey (MGRS).

angular sizes of nearby galaxies, while the faint end is chosen to match the magnitude limit of the SDSS main galaxy sample. In addition, we also include galaxies with $0.01 \leq z \leq 0.2$ in the NYU-VAGC that have redshifts from alternative sources: 2dFGRS (Colless et al. 2001), the PSCz (Saunders et al. 2000) or RC3 (de Vaucouleurs et al. 1991). Our final sample consists of 286563 galaxies. In our analysis, we construct two volume-limited samples in two bins of the absolute magnitude $^{0.1}\mathrm{M}_r - 5\log h$: V1 (-22.0, -20.5] and V2 (-22.0, -21.0] (see Table 1 for the detailed selection criteria). Note that these two volume-limited galaxy samples are different from those used in constructing the group catalogues, and are used only in measuring the cross correlations.

2.2. *Mock Samples of Galaxies*

In order to check how accurately our methodology allows us to detect true effects of assembly bias, we construct a mock galaxy redshift survey (MGRS) that incorporates the same observational selection effects as the SDSS sample. Our MGRS is based the model galaxy catalogue constructed by Croton et al. (2006) using a semi-analytic model of galaxy formation in combination with the 'Millennium Run' N-body simulation (Springel et al. 2005) [7]. The cosmological parameters adopted in the 'Millennium Run' are $\Omega_m = 0.25$, $\Omega_\Lambda = 0.75$, and a CDM spectrum with an amplitude specified by $\sigma_8 = 0.9$. The simulation was performed with the code GADGET2 (Springel et al. 2005), using 2160^3 dark matter particles in a periodic cubic box with a side length $L_{\rm box} = 500\,h^{-1}$Mpc (in comoving units). The mass of a particle is $8.6 \times 10^8\,h^{-1}\mathrm{M}_\odot$. The galaxy catalogue is generated based on a semi-analytical model of galaxy formation which uses the simulated halo merging trees. We refer the reader to Croton et al. (2006) for the details of the semi-analytic model. Because of the finite mass resolution in the simulation, the sample is complete to a luminosity limit $^{0.1}\mathrm{M}_r - 5\log h \sim -16.6$.

Our construction of the MGRS here is similar to that described in Li et al. (2007a; see also Yang et al. 2004).

[7] http://www.mpa-garching.mpg.de/galform/agnpaper

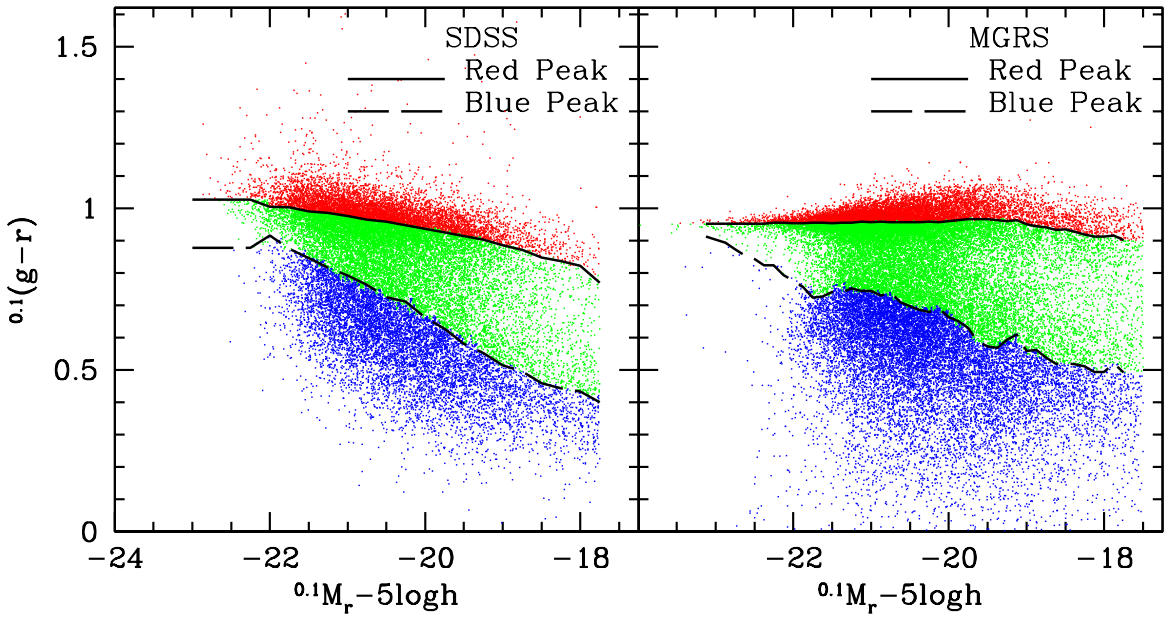

FIG. 1.— The color-magnitude distributions of galaxies in the SDSS (left-hand panel) and the MGRS (right-hand panel). The dotted- and dashed- lines indicate the centers of the two Gaussian used to describe the color distributions at a given luminosity bin (see text for details). These are used to split the galaxy populations in red (above the red sequence), blue (below the blue sequence) and green (in between the red and blue sequences). For clarity, only 10% of all galaxies in the SDSS and MGRS are shown.

First, we stack $3 \times 3 \times 3$ replicates of the simulation box and place a virtual observer at the center of the stacked boxes. Next, we assign each galaxy a (α, δ)-coordinate and remove the ones that are outside the mocked SDSS survey region. For each model galaxy in the survey region, we compute its redshift (which include the general expansion, the peculiar velocity, and a $35\,\mathrm{km\,s^{-1}}$ Gaussian line-of-sight velocity dispersion to mimic the redshift errors in the data), its r-band apparent magnitude (based on the r-band luminosity of the galaxy), and its absolute magnitude $^{0.1}\mathrm{M}_r - 5\log h$ which is $K+E$ corrected to $z = 0.1$. We eliminate galaxies that are fainter than the SDSS apparent-magnitude limit, and incorporate the position-dependent incompleteness by randomly eliminating galaxies according to the completeness factors obtained from the survey masks that are provided by the NYU-VAGC (Blanton et al. 2005b). Finally we select the same two volume-limited samples (V1 and V2) from the MGRS as we used for the actual data. The numbers of (mock) galaxies in these two samples are listed in the last column of Table 1. Note that they do not match the SDSS data perfectly. This mainly owes to the fact that the semi-analytical model does not match the observed luminosity function perfectly.

2.3. *Random Samples of Galaxies*

In order to measure the two-point correlation functions, one needs to construct random samples to normalize the pair counts. To do this, we first generate a set of random 'galaxies' according to the luminosity function obtained by Blanton et al. (2003b). Here a large set of points are randomly distributed within the survey sky coverage and each point is assigned a redshift and an absolute magnitude according to the luminosity function. The redshifts are assigned to random galaxies by assuming that they have a constant number density as a function of redshift. Similar to the last step in constructing the MGRS, we apply the completeness and magnitude limit according to the survey masks provided by Blanton et al. (2005b). The total number of 'galaxies' in each random sample is about 7.5 times as large as that in the corresponding observational or mock sample.

2.4. *Galaxy Group Samples*

Our analysis is based on the group catalogue of Yang et al. (2007), which is constructed from the SDSS Data Release 4 using a modified version of an adaptive halo-based group finder (Yang et al. 2005a). This group finder is optimized to assign galaxies into groups according to their common dark matter halos. Each group is assigned two values of halo mass, one is based on the ranking of group characteristic luminosity and is referred to as the luminosity-based halo mass (M_L), and the other is based on the total stellar mass of the group and is referred to as the stellar mass-based halo mass (M_S) (see Yang et al. 2007 for details). Note that this method requires knowledge of the halo mass function, and is therefore cosmology dependent.

In this paper, we measure the galaxy-group cross-correlation function (hereafter GGCCF) to quantify the dependence of the clustering on group mass and on the color of the group members. To this end, we divide galaxy groups into four samples according to their halo masses. The criteria used to define these samples are listed in Table 2. We further divide each of the group samples into color subsamples using either the color of the central galaxy (C0) or using the total color of all group members (C1). Below we describe these color subsamples in more detail.

- **C0 subsamples:** based on the color of the central galaxy. Here, the central galaxy of a group is defined to be the brightest member in the group, and we assume that the location of the central galaxy coincides with the center of mass of the group. Tests show that our results do not change signif-

icantly if the central galaxy is defined to be the most massive group member instead. Note that only a very small portion ($\lesssim 0.6\%$) of groups in which the most massive galaxy is different from the brightest galaxy. Recent investigations of the color-magnitude distribution of galaxies show that the colors of galaxies for a given absolute magnitude follows a bi-normal form (e.g., Baldry et al. 2004; Blanton et al. 2005a; Li et al. 2006). Following Li et al. (2006), we separate the SDSS galaxies into 118 bins according to their absolute magnitudes, ${}^{0.1}\mathrm{M}_r - 5\log h$, and fit the ${}^{0.1}(g-r)$ color distribution in each bin using a double-Gaussian function. The centers of the Gaussians are shown in the left-hand panel of Fig. 1 as solid and dashed lines, and are used the split the galaxy population in red (above solid line) blue (below dashed line) and green (in between the solid and dashed lines) subsamples. Using the color of the central galaxies, we also split the group catalogue in red, blue and green subsamples. The mean colors of the central galaxies in each subsample are listed in columns 4 - 6 of Table 2.

- **C1 subsamples:** based on the total color of each group. In this case, we first add up the r-band and g-band luminosities of all member galaxies for each group to get the total group luminosity $L_{r,t}$, $L_{g,t}$, respectively. The groups are then separated into red and blue subsamples of equal size (i.e., with equal numbers of groups) according to the group color $2.5*(\log L_{r,t} - \log L_{g,t})$. The mean colors of the groups in each subsample defined in this way are listed in columns 7 and 8 of Table 2.

We have also selected galaxy groups from the MGRS using exactly the same group-finding algorithm as applied to the real sample (see Yang et al. 2007 for more details). Here again we assign to each selected group two values of mass, one (M_L) based on the characteristic group luminosity and the other (M_S) based on the group stellar mass. The groups selected from the MGRS are also divided into samples of different masses and into subsamples according to the color of the central galaxy and according to the total group color, respectively. The information about about these samples can be found in Table 3 with the same format as in Table 2. When modeling the color-magnitude distribution of the mock galaxies, we separate the galaxies into 113 bins of ${}^{0.1}\mathrm{M}_r - 5\log h$ and fit the ${}^{0.1}(g-r)$ color distribution in each bin with a double-Gaussian function. The right-hand panel of Fig 1 shows the two ridges defined by the peaks of the double-Gaussian function. As for the SDSS data, these ridges again are used to separate galaxies into red, green and blue subsamples.

3. THE GROUP-GALAXY CROSS-CORRELATION FUNCTION

In this paper, we use the group-galaxy cross correlation function (hereafter GGCCF) to study the clustering of galaxy groups in the galaxy density field. We choose to use the cross correlation instead of the auto-correlation, because in this case much larger number of galaxies (compared to the number of groups) can be used as tracers of the underlying density field, allowing a more accurate determination of the correlation strength of the groups. We estimate the GGCCF in redshift space using the definition proposed in Davis & Peebles (1983),

$$\xi(s) = \frac{CG(s)\ n_R}{CR(s)\ n_G} - 1\,, \tag{1}$$

where CG is the count of group-galaxy pairs between a group sample and the corresponding galaxy sample; CR is the count of group-'random' pairs between a group sample and the corresponding random 'galaxy' samples; s is the separation of the pairs in redshift space; n_G and n_R are the number densities of the galaxy sample and the random sample, respectively. Group-galaxy and group-random pairs are counted in logarithmic bins in s, with bin width $\Delta\log_{10}(s) = 0.14$. Note that the redshift-space correlation function is not linearly proportional to the bias of the groups. Indeed, the large-scale redshift-space mono-pole of the auto correlation function is

$$\xi(s) = \xi(r) * f(\beta) = \xi(r) * (1 + 2/3\beta + \beta^2/5) \tag{2}$$

where $\beta = \Omega_m^{0.6}/b$. So the amplitude of $\xi(s)$ increases less rapidly with halo mass than $\xi(r)$. Assuming $\Omega_m = 0.25$, the difference in $f(\beta)$ between $b = 1$ and $b = 2$ is 1.33 to 1.15, respectively. Thus, we caution that the relative bias measured from the $\xi(s)$ may be underestimated by a few percent ($\lesssim 1 - \sqrt{1.15/1.33}$).

We also estimate the projected GGCCF, defined as

$$W(r_p) = 2\int_0^\infty \xi(r_p, r_\pi) dr_\pi = 2\sum_k \xi(r_p, r_{\pi,k})\Delta r_{\pi,k}\,. \tag{3}$$

where $\xi(r_p, r_\pi)$ is the GGCCF defined in a similar way to Eq. (1), but as a function of the separations of group-galaxy pairs perpendicular (r_p) and parallel (r_π) to the line-of-sight. Here, group-galaxy and group-random pairs are counted in logarithmic bins in r_p, with a bin width $\Delta\log_{10}(r_p) = 0.17$, and in linear bins of r_π, with a bin width $\Delta r_\pi = 1\,h^{-1}$Mpc. In practice, the summation in (3) is carried over k from 1 to 40, corresponding to $0 \le r_\pi \le 40\,h^{-1}$Mpc.

Since we have two galaxy samples V1 and V2, we can make different combinations of the group and galaxy samples so that the depths of the samples to be cross correlated match the best. Unless stated otherwise, we will use V1 to cross-correlate with the group samples G1 and G2 (or S1 and S2), while we use V2 to cross-correlate with the group samples G3 and G4 (or S3 and S4).

We estimate the errors of the GGCCF using the bootstrap resampling method (Barrow, Bhavsar, & Sonoda 1984; Mo, Jing & Börner 1992). We compute the GGCCFs for 100 bootstrap samples of both galaxies and groups (either real or mock), and estimate the errors from the scatter among these GGCCFs. For this purpose, we measure the covariance matrix of the GGCCF, which is then diagonalized. Throughout the paper we use the diagonalized terms of the covariance matrix to plot the error bars.

4. RESULTS FROM THE OBSERVATIONAL SAMPLES

4.1. *The Dependence of the Group-Galaxy Cross-Correlation on Group Mass*

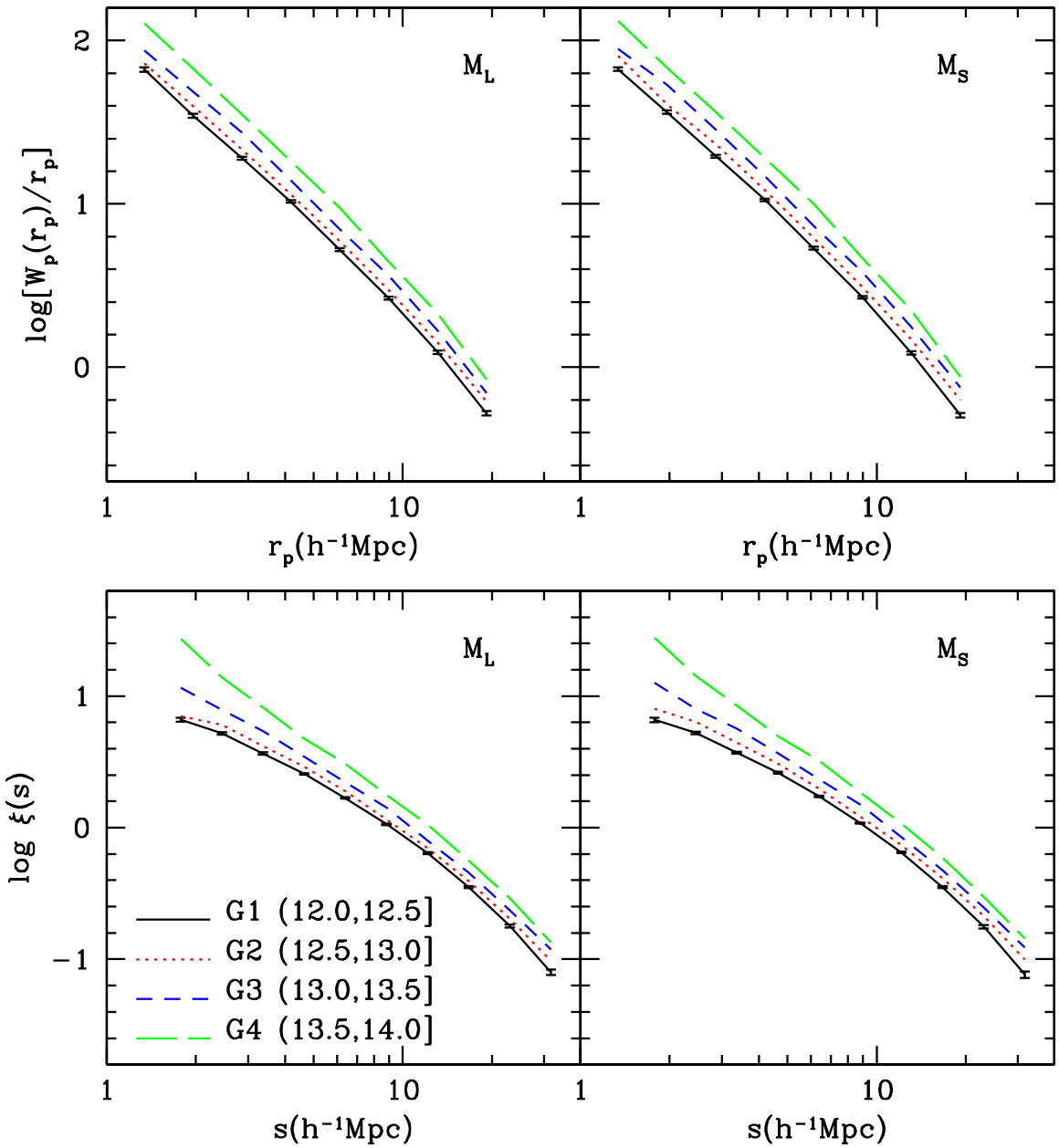

FIG. 2.— Upper panels: the projected GGCCF between the volume-limited galaxy sample V2 (-22.0, -21.0] and the group samples (G1-G4) within different mass ranges as indicated. Lower panels: similar to the upper panels, but for GGCCF measured in redshift space. In the plot, M_L (left panels) and M_S (right panels) correspond to groups with masses that are estimated from the ranking of group luminosity and stellar mass, respectively.

We start by examining how the group-galaxy cross-correlation depends on group mass. To this extent, we measure the projected and redshift-space GGCCFs between group samples G1-G4 and the volume-limited galaxy sample V2. The corresponding results are shown in Fig. 2. Upper and lower panels correspond to the projected GGCCFs and redshift-space GGCCFs, respectively. Results are shown for both group mass estimates, M_L and M_S, separately in the left and right-hand panels, respectively. Clearly, the GGCCFs for more massive groups have higher amplitudes, although their shapes are similar on large scales. Since the same galaxy sample is used for all these GGCCFs, this implies that more massive groups are more strongly correlated in the galaxy density field. Note also that the results for M_L and M_S are very similar, indicating that they do not depend strongly in which mass indicator we use.

To quantify the mass-dependence of the cross correlation amplitude, we measure the relative clustering bias for groups of different masses. We obtain the relative bias using the average ratio of the GGCCFs in the range $4.19\,h^{-1}$Mpc $\leq r_p \leq 19.17\,h^{-1}$Mpc or $4.64\,h^{-1}$Mpc $\leq s \leq 22.98h^{-1}$Mpc between group samples Gi (i=1,4) and G1. In Fig. 3, we show the relative bias measured from the projected (left panel) and the redshift-space (right panel) GGCCFs, as function of halo mass. The increase of the bias with group mass can be well modeled with a quadratic function, which is also shown in the figure. We compare the observed bias - mass relation with the prediction of the halo bias model of Sheth, Mo & Tor-

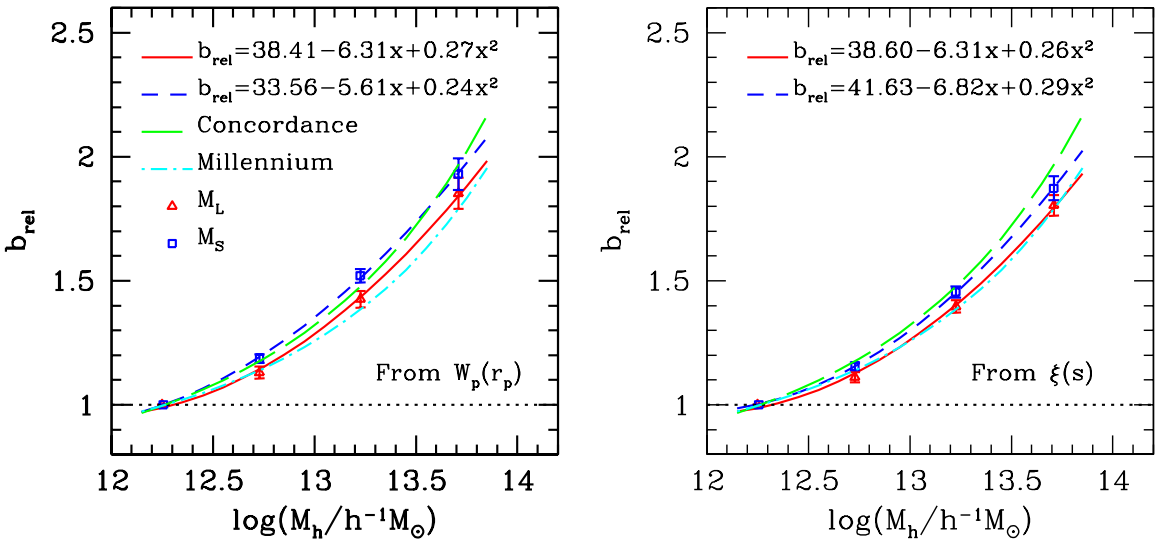

FIG. 3.— Left panel: The average relative bias parameters, obtained from the projected GGCCFs in the range $4.19\,h^{-1}$Mpc $\leq r_p \leq$ $19.17\,h^{-1}$Mpc shown in the upper panels of Fig. 2, as a function of group mass M_L (triangles) and M_S (squares). The error bars are measured based on the 1-σ variances of 100 bootstrap re-samplings. The relative bias parameters are normalized by the projected GGCCF of the group sample G1. The solid curve shows the best fitting to the relative biases of groups with mass M_L (triangles). While the dashed curve is the best fitting relative biases for groups with mass M_S (squares). Right panel: The same as the left panel, but for relative bias parameters obtained using the GGCCFs in redshift space, i.e. the data shown in the lower panels of Fig 2 in the range $4.64\,h^{-1}$Mpc $\leq s \leq 22.98\,h^{-1}$Mpc. The corresponding best fitting results are plotted as the solid and dashed lines respectively. We also show the relative biases obtained from the halo model predictions (Sheth, Mo & Tormen 2001) for the cosmologies we adopted for the SDSS observation $[\Omega_m, \Omega_\Lambda, \sigma_8] = [0.24, 0.76, 0.77]$ and the Millennium simulations $[\Omega_m, \Omega_\Lambda, \sigma_8] = [0.25, 0.75, 0.9]$ respectively using long-dashed and dot-dashed lines.

men (2001), adopting the same cosmology as used in the construction of the group catalogue (Yang et al. 2007) (the long-dashed line), and adopting the same cosmology as used in the 'Millennium Run' simulation (dot-dashed line). As one can see, the observed relation is well reproduced by the model, but it does not allow us to discriminate between these two cosmological models. These results are all in excellent agreement with those obtained by Yang et al. (2005b) based on the groups selected from the 2dFGRS.

4.2. *The Dependence on Group Color*

Next we investigate how the GGCCF depends on the colors of the galaxies in the groups. We first consider the case C0 described above, in which the color of a group is defined by the color of its central galaxy. We measure the projected GGCCFs between the groups with all, red, green or blue centrals and the galaxy samples V1 or V2. The relative bias for each case is then obtained from the ratio between the projected GGCCF of the case in question and that of the groups with all centrals. The resulting relative bias, $b_{\rm rel}$, is shown as a function of r_p in Fig. 4. The four different panels correspond to four different group mass bins, G1 - G4, as indicated, where group masses are based on M_L. The relative bias relations for groups with red, green and blue centrals are plotted as dotted, long-dashed and dashed lines, respectively. In order to obtain better statistics, the projected GGCCFs are measured between the following pairs of group-galaxy samples: G1-V1; G2-V1; G3-V2 and G4-V2. Note that in general groups with red centrals are more strongly clustered than groups of the same mass but with blue centrals. The effect is somewhat stronger at smaller separations and for less massive groups. Groups with green centrals show no significant bias relative to the total population.

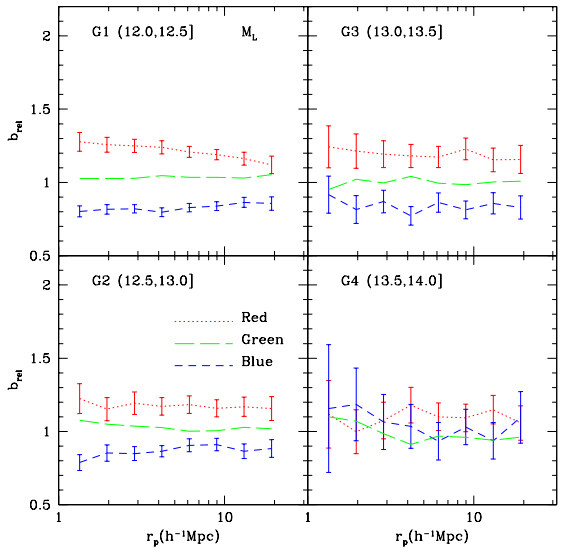

FIG. 4.— The relative biases $b_{\rm rel}$ as a function of r_p obtained from the ratios of the projected GGCCFs of groups with red, green and blue central galaxies to that of all groups in different group mass bins as indicated. In this plot, the group masses, M_L, are estimated using the ranking of the characteristic group luminosity.

We can also measure the relative bias using the GGCCFs in redshift space. Fig. 5 shows this relative bias, $b_{\rm rel}$, as a function of the redshift-space separation s. The overall behavior of the color dependence of the relative bias obtained here is very similar to that shown in Fig. 4.

Note that the results presented in Figs. 4 and 5 are based on the halo mass estimate M_L. It is interesting to compare these with the results obtained using the mass estimate M_S. Since red groups have larger stellar masses than blue groups of the same luminosity, these two estimates of halo masses, M_L and M_S, may

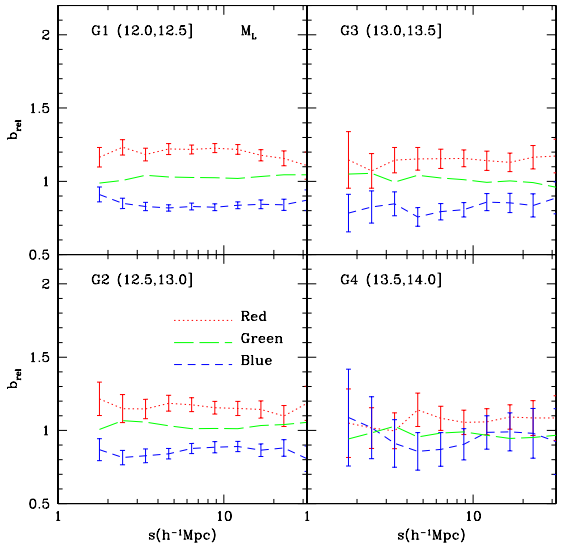

FIG. 5.— The same as Fig. 4, except that the relative biases $b_{\rm rel}$ are obtained from the redshift space GGCCFs and shown as function of s.

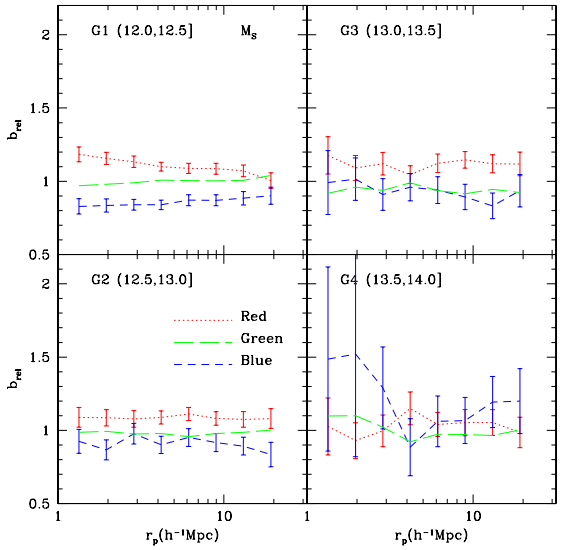

FIG. 6.— Similar to Fig. 4, but for groups with masses, M_S, estimated from the ranking of the characteristic stellar masses of the groups.

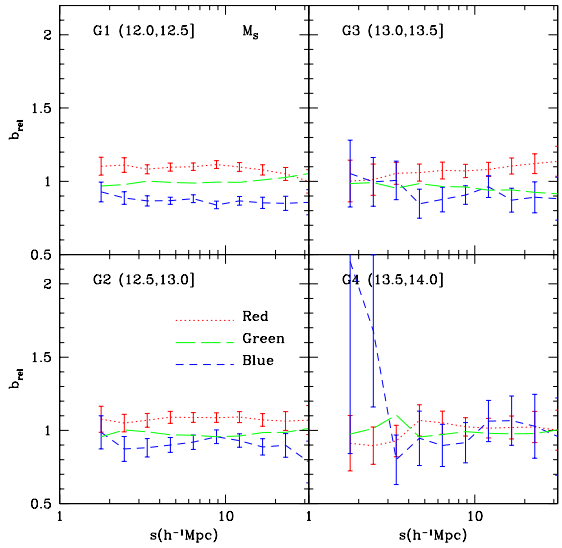

FIG. 7.— Similar to Fig. 5, but for groups with masses, M_S, estimated from the ranking of the characteristic stellar masses of the groups.

be systematically different for red and blue groups of the same luminosity, which may affect the color dependence of the GGCCF discussed above. In Figs. 6 and 7 we show the relative bias of groups of different color properties against the projected separation r_p and redshift-space separation s for groups with similar M_S. The color dependence of $b_{\rm rel}$ is clearly significant for groups with $M_S \lesssim 10^{13.5} h^{-1}{\rm M}_\odot$, though it is weaker than that shown in Figs. 4 and 5. This can be explained as follows. Because M_L is smaller than M_S for redder groups, for a given mass bin, the average value of M_S of the redder subsample defined by M_L is larger than that defined by M_S. Consequently, the bias of the redder subsample is boosted in the M_L sample because of the increased halo masses. Although M_S is arguably a better estimate of the halo mass (see Yang et al. 2007), the difference in the color dependence of the bias due to the use of different halo mass estimates suggests that further tests are required to assess the reliability of our results. We will return to this in the next section.

To quantify the dependence of the relative bias $b_{\rm rel}$ on the color of the central galaxy, we calculate the average relative bias factor for groups in each mass bin based on the projected GGCCF over the range $4.19\ h^{-1}{\rm Mpc} \leq r_p \leq 19.17\ h^{-1}{\rm Mpc}$, and the corresponding bias factor based on the redshift-space GGCCF over the range $4.64 h^{-1}{\rm Mpc} \leq s \leq 22.98 h^{-1}{\rm Mpc}$. The results are shown in Fig.8. The upper two panels show the relative biases for groups with halo masses based on M_L, while the lower two panels are those for groups with halo masses based on M_S. The left two panels are results obtained from the projected GGCCFs, while the right panels are results obtained from the redshift-space GGCCFs. The related error bars are estimated from the 1-σ variances of the 100 bootstrap re-samplings. Note that the average masses of groups are slightly different when the group samples G1 - G4 are divided into color subsamples. To take care of the contamination due to such mass difference, we have corrected the relative bias of the color subsamples relative to the whole sample, using the mean relation shown in Fig. 3 according to the average $\log M_h$ of the subsample in question. Such correction is applied throughout when we examine the color dependence of the relative bias.

As one can see from Fig. 8, at a fixed group mass, the relative bias of groups with red centrals is higher than that of groups with blue centrals. The color dependence is more significant for groups of lower masses, and becomes insignificant in massive groups with $M \gtrsim 10^{13.5}\ h^{-1}{\rm M}_\odot$. As already eluded to above, the results obtained from the projected and redshift-space GGCCFs are very similar, while the color dependence is weaker when using M_S to estimate group masses than when using M_L. Note that as we will show in the next section part of the color dependence is induced by systematic error, which is stronger for group mass M_L. To illustrate to what extent the color-dependence of the group clustering can be compared with the age-dependence of halo clustering, we show, as the dot-dashed and dot-long-dashed lines, in the lower left panel

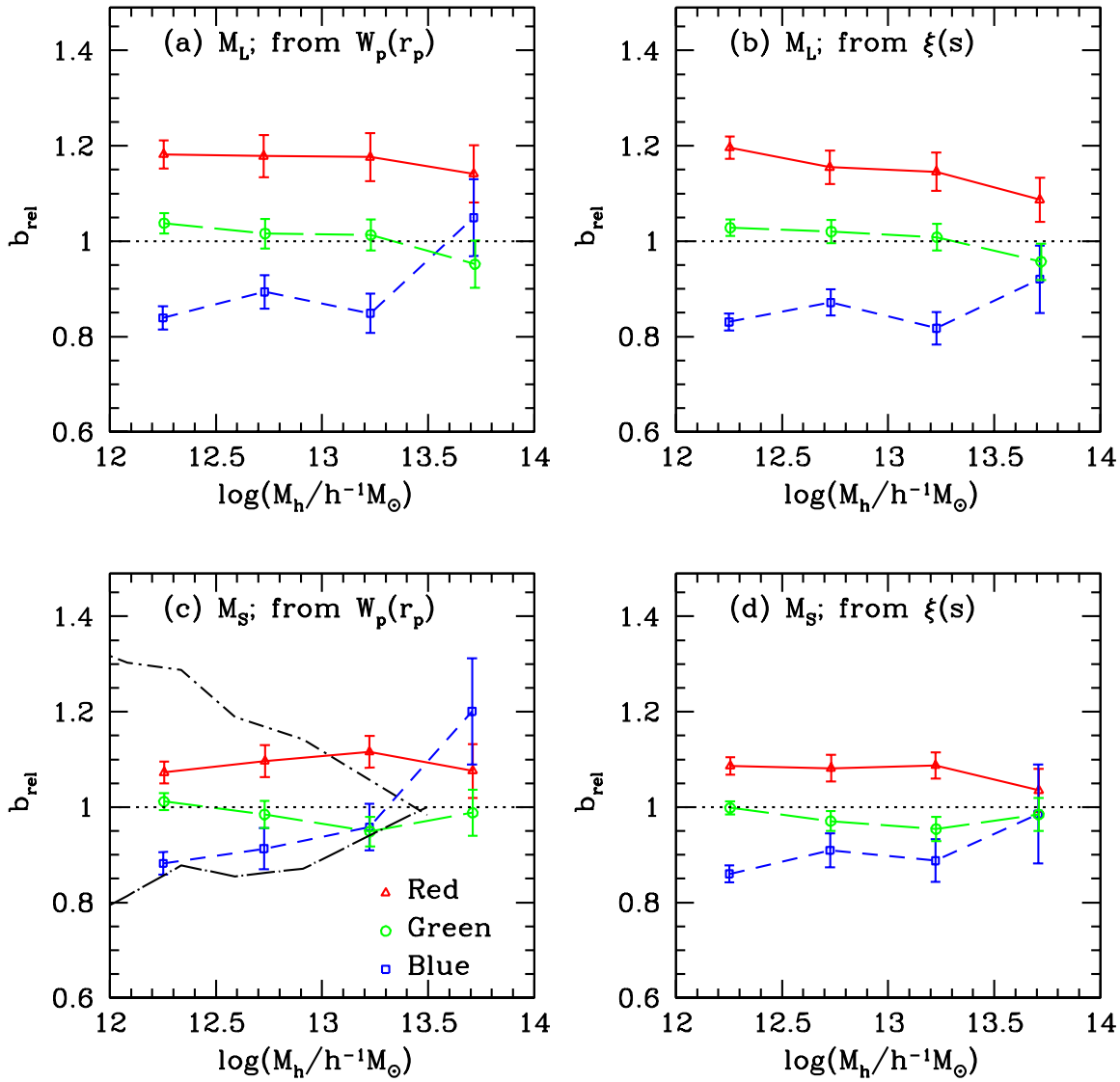

FIG. 8.— Panel (a): the average relative biases as a function of halo mass (for M_L) obtained from the projected GGCCFs shown in Fig. 4 in the range $4.19\,h^{-1}$Mpc $\leq r_p \leq 19.17\,h^{-1}$Mpc. Panel (c): similar to panel (a), but for groups with halo masses M_S. Panel (b): the average relative biases as a function of halo mass (for M_L) obtained from the redshift space GGCCFs shown in Fig. 5 in the range $4.64\,h^{-1}$Mpc $\leq s \leq 22.98\,h^{-1}$Mpc. Panel (d): similar to panel (b), but for groups with halo masses M_S. In each panel, we show the relative biases for groups with red, green and blue central galaxies using open triangles, squares and circles, respectively. For comparison we show also in the lower-left panel the age dependence of the halo clustering obtained by Gao et al. (2005) from N-body simulations. The dot-dashed and dot-long-dashed lines correspond to relative biases for the 20% old and young halos with respective to all halo populations, respectively.

of Fig. 8 the results for the 20% oldest and the 20% youngest halos obtained by Gao et al. (2005). The color-dependence of the group clustering is qualitatively similar to the age-dependence of the halo clustering. Quantitatively, however, while groups with blue centrals have relative bias similar to that of young halos, the bias for low-mass groups with red central galaxies is significantly lower than that of low-mass old halos. Thus, the color of the central galaxy and the assembly history of the host halo is correlated, but the relation contains a large random component.

Following Berlind et al. (2006a), we also determine the dependence of the relative bias on the overall group color (using the C1 subsamples defined in section 2.4). The average relative biases of red and blue groups thus defined are plotted in Fig. 9 as a function of halo mass[8]. A comparison with Fig. 8 shows that the color dependence of the relative bias based on C1 is weaker than that based on C0. The main reason for this is that in C0 groups are separated into three color subsamples, while only two subsamples are used in C1. Consequently, the red and blue subsamples in C0 are further separated in color-space than those in C1 (cf. Table 2).

All these results regarding the color dependence of the halo bias are in good, qualitative agreement with those obtained by Yang et al. (2006) from the 2dFGRS, as long as red galaxies are mainly the galaxies with passive star formation. However, they are completely opposite

[8] For completeness, we have also determine the relative biases using the *average* colors of the group members, rather than the total colors, which yields results that are virtually indistinguishable

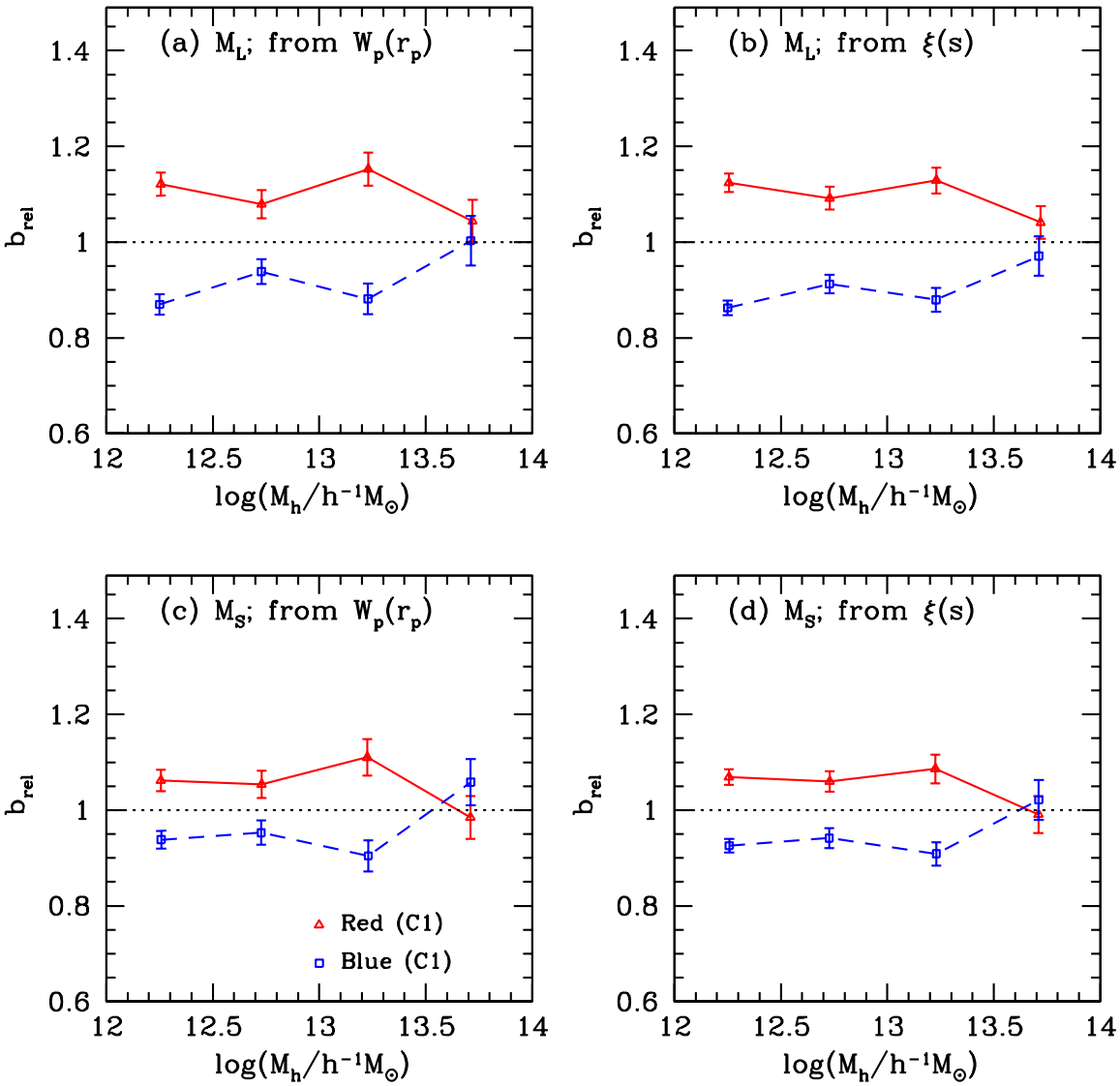

FIG. 9.— Panel (a): The average relative bias, obtained using the projected GGCCFs in the range $4.19\,h^{-1}$Mpc $\leq r_p \leq 19.17\,h^{-1}$Mpc for red and blue groups in terms of C1 and C2 as indicated. In this panel the groups masses, M_L, are estimated according to the ranking of characteristic group luminosity. The error bars are estimated from 1-σ variances of the 100 bootstrap re-samplings. The relative bias parameters of red and blue groups are normalized by the projected GGCCFs of all groups in the corresponding mass bin. Panel (b): Similar to panel (a) but for relative biases measured from the redshift space GGCCFs in the range $4.64\,h^{-1}$Mpc $\leq s \leq 22.98\,h^{-1}$Mpc. Panels (c) and (d): Similar to panels (a) and (b), but for groups with masses, M_S, estimated using the ranking of characteristic group stellar masses.

to the results obtained by Berlind et al. (2006a) who, using the SDSS group catalogue of Berlind et al. (2006b), found that (i) blue groups are more strongly clustered than red groups of the same mass, and (ii) the color dependence is stronger for more massive groups. Since the galaxy samples and statistical methods used are very similar, these differences more likely result from differences in the group-finding algorithms used or the groups selected. The general properties of the groups selected by Berlind et al. are similar to the groups used here. For instance, relationship between group richness and halo mass is about the same for both group catalogs. However, we do find that the central galaxy luminosity - halo mass relation in their group samples is quite different from that in ours, particularly for groups with masses $\lesssim 10^{13.5}\,h^{-1}\mathrm{M}_\odot$. In their Fig. 3(d), Berlind et al. (2006a) showed that the central galaxies in low-mass halos have three or four distinctive populations (with unfilled gaps), which are not present in our samples. Thus the groups, especially the low-mass ones, are somewhat different in the two catalogs. On the other hand, as we will show in the next section using mock samples, the use of M_L as group mass induces systematic errors that can produce a significant part of the observed color dependence of the clustering bias factor. Since Berlind et al. have also used the group masses estimated using the total group luminosities, their results might also be affected by such systematic effect. Unfortunately, the bias due to the systematic effect is expected to be in the opposite direction as color-dependence found by Berlind et al. (2006a), namely, it should enhance the clustering amplitude of red groups. While it is beyond the scope of our paper to identify in detail the origin of the discrepancy, we use mock samples in the next section to test the reliability of our results.

Before proceeding to the next section, we follow

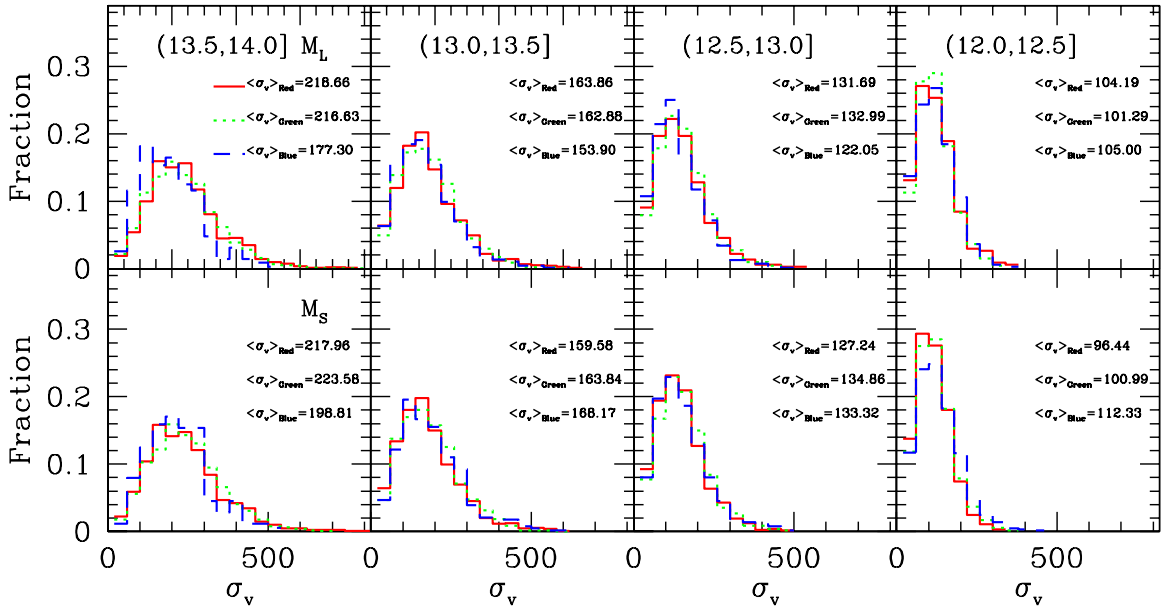

FIG. 10.— The distribution of the velocity dispersions for groups with red, blue and green centrals as indicated. The panels from left to right correspond to groups of different masses. The upper and lower panels show the results with M_L and M_S as the group mass, respectively. The velocity dispersions are estimated for groups with at least two members.

Berlind et al. (2006a) to check whether the velocity dispersions of the groups in halos of the same assigned mass but with centrals of different colors are the same. This provides yet another test about the reliability of our mass assignment. Here we measure the velocity dispersions for groups with at least two members using the gapper estimator described by Beers, Flynn & Gebhardt (1990; see also Yang et al. 2005a). Although the estimate of the velocity dispersion is unreliable for estimating individual halo mass, the stacking result may be a reliable indicator of the mean mass of a set of groups. To show that the color-dependent bias is not a result of systematic mass difference between the color subsamples, we estimate the mean velocity dispersion of each color subsample. The results are shown in Fig. 10 for groups of different assigned masses, with upper and lower panels corresponding to masses based on M_L and M_S, respectively. The results show clearly that there is no systematic difference between the mean velocity dispersions of groups with red, blue and green centrals. Thus, the color dependence we found in the SDSS observation is unlikely due to systematics in the mass assignments.

5. RESULTS FROM THE MOCK SAMPLES

In this section, we use the MGRS constructed from the Millennium semi-analytical galaxy catalogue (Croton et al. 2006) to investigate the mass and color dependence of the GGCCF. The purpose here is twofold. First of all, as mentioned above, we want to test the reliability of our results against uncertainties in the identification of galaxy groups, and in the mass assignments. Secondly, we also want to investigate whether the semi-analytical model of Croton et al. which is fairly successful in matching observational data, actually predicts a color dependence of the halo bias and how it compares to the data presented here.

5.1. *Dependence on Group Mass*

The GGCCFs for the MGRS have been measured using exactly the same method used in Section 4.1 for the real data. Fig. 11 shows the GGCCFs for mock groups in different mass bins. Comparing these results with the observational results shown in Fig.2), one sees that the mass dependence predicted by the model is very similar to that obtained from the SDSS. Fig. 12 shows the corresponding relative bias as a function of group mass. As in the observational data, the relative biases are defined with respect to groups with masses in the range $10^{12.0} - 10^{12.5}\,h^{-1}\mathrm{M}_\odot$. The mass dependence of the relative bias can again be modeled with quadratic forms, as indicated in the panels. As with the SDSS data, the results are well matched by the predictions based on the clustering of dark matter halos in a ΛCDM cosmology, suggesting that our group finder is quite reliable in grouping galaxies according to their common dark matter halos. In addition, the halo masses assigned to the groups also have to be fairly reliable, otherwise we would not have been able to recover the strong mass dependence shown. This is also consistent with the tests described in Yang et al. (2007), where it is shown that the masses assigned to the groups agree with the true halo masses with a scatter $\lesssim 0.3$ dex.

5.2. *The Dependence on Group Color*

Fig.13 shows the relative biases of red, green and blue groups in the MGRS as function of the assigned group mass. Here the colors refer to those of the central galaxies (i.e., the brightest group members), which have been determined using the color-magnitude relation shown in the right-hand panel of Fig. 1. As for the real data, the relative bias is defined relative to the GGCCF of all groups in the mass bin. In the left-hand panels the relative biases have been estimated from the projected GGCCFs using the data over the range $4.19\,h^{-1}\mathrm{Mpc} \leq r_p \leq 19.17\,h^{-1}\mathrm{Mpc}$. The right-hand panels shows the relative bias factors obtained from the redshift-space GGCCFs using the data in the range

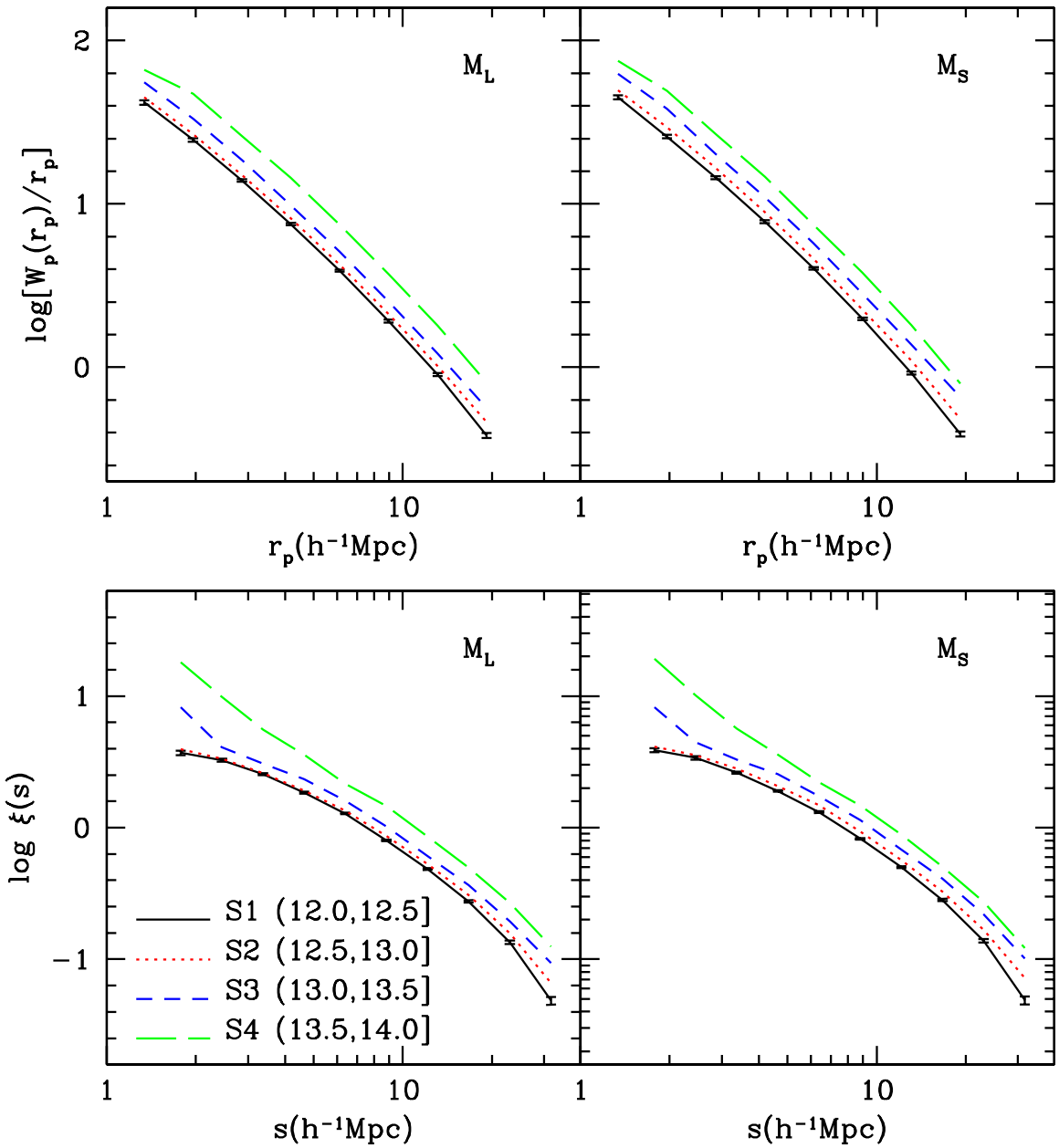

FIG. 11.— Similar to Fig. 2, except that the results are for the MGRS constructed from the Millennium galaxy catalogue.

$4.64\,h^{-1}$Mpc $\leq s \leq 22.98\,h^{-1}$Mpc. The results shown in the upper two panels use group masses based on M_L, while the lower two panels use group masses based on M_S. Compared with the observational results shown in Fig. 8, the MGRS reveals a significantly stronger color dependence, especially for groups in the lowest mass bin, $10^{12.0} - 10^{12.5}\,h^{-1}\mathrm{M}_\odot$.

In order to investigate to what extent this color dependence of the GGCCF is affected by selection effects, we compare the results obtained from the MGRS with those obtained directly from the Millennium galaxy catalogue. For this purpose, we measure the relative biases directly from the Millennium simulation and use the color of the central galaxy to separate halos of a given mass into red, green and blue subsamples. Here we use the auto-correlation function of the dark matter halos (instead of the GGCCF) *in real space* to estimate the relative bias of halos in different subsamples. The relative biases are defined relative to the correlation function of all groups in the mass bin in question, and are estimated using data in the separation range $8.98h^{-1}\mathrm{Mpc} \leq r \leq 44.6h^{-1}\mathrm{Mpc}$. The solid symbols in Fig. 13 show the relative bias factors of red, green and blue halos thus obtained as function of the true halo mass. Clearly, the SAM predicts a color dependence. Similar to our results, red halos are more strongly clustered than blue halos of the same mass, and the color dependence is stronger for less massive halos. A comparison with the corresponding open symbols, which show the results obtained from the mock group catalogue constructed from the MGRS, indicates that the color dependence in the original data is fairly well recovered by our analysis of the GGCCF. In particular, when using M_S as halo mass estimator, the true trends can be recovered fairly accurately. Quantitatively how-

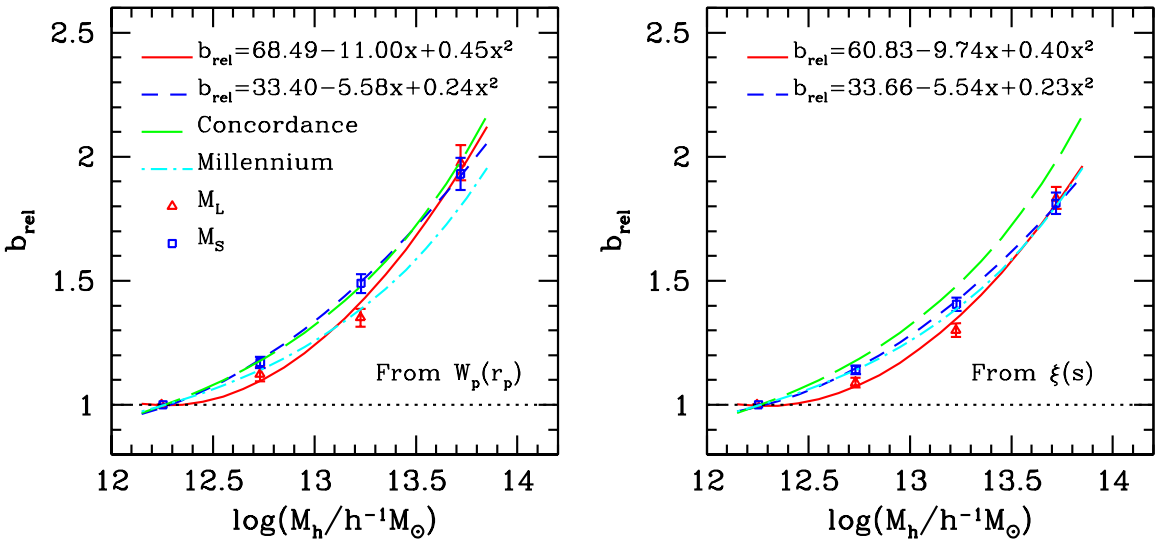

FIG. 12.— Similar to Fig. 3, except that the results are for the MGRS constructed from the Millennium galaxy catalogue.

ever, there is discrepancy between the original signal in the Millennium Simulation and that recovered from the mock groups, especially for blue groups when GGCCFs in redshift space are used, in the sense that the recovered color dependence is stronger than the dependence in the original data. The discrepancy is larger when M_L is used. The amount of systematics is comparable to the difference between red and blue groups in the observational sample [see panels (c) and (d) of Fig.8]. In order to check further how the color dependence of the group clustering in the SDSS data can be affected by the group finder used and the model of halo-mass assignments, we carry out an additional test. Here we first randomly re-assign to each central or satellite galaxy of a given stellar mass in the Millennium Simulation a $^{0.1}(g-r)$-color according to the color-stellar mass relation of the central or satellite galaxies in the SDSS observation. The absolute magnitude of each mock galaxy is then re-calculated according to the new assigned color. Note that such a color assignment according to the SDSS observation makes sure that the color distribution of mock galaxies is the same as that in the observation, thereby reducing any effects that may be produced by the difference in the color distribution. Thus, the re-constructed new mock galaxy catalogue has a similar color-stellar mass relation as the SDSS observation. More importantly, there should not be any color-dependence of group clustering in this new mock catalog. Using this catalogue, we generate the MGRS again and perform all the same analyses (i.e. finding groups, assigning halo masses according to luminosity or stellar mass, and calculating the group correlation function) to obtain the relative bias of corresponding galaxy groups. The results are shown in Fig. 14 as the open symbols for groups with red (triangles), green (circles) and blue (squares) central galaxies, defined with the color criteria that is exactly the same as in the observation. For comparison, we also show, as the solid symbols, the true relative bias based on the original *halos* in the MGRS. The use of halos in the *MGRS* ensures that we are comparing the *same* set of halos (groups) in the same large-scale structures and the differences between the two are simply due to the systematic errors. Ideally, the relative biases for the halos in the MGRS should contain no color dependence, and the deviation of the solid symbols from the null hypothesis, $b_{rel} = 1$, which is at roughly the 1-σ level, reflects the 'cosmic variance' in the color assignment. As can be seen, there is some difference between the open and solid symbols, which indicates the systematic errors introduced by the group-finding procedure and the halo-mass assignment. The systematic errors are $\lesssim 0.1$ for the cases using M_L (see the upper two panels of Fig. 14), and are $\lesssim 0.05$ for the cases using M_S (see the upper two panels of Fig. 14). These are significantly smaller than the difference shown in Fig. 8. Finally we have also made a test in which each central or satellite galaxy in the Millennium Simulation is randomly re-assigned a $^{0.1}(g-r)$ color according to the color-*magnitude* relation of the central or satellite galaxies in the SDSS. The overall systematics here is slightly smaller. Based on all these tests with the mock catalog, we conclude that our results are robust against the systematics produced by the group-finding procedure and the halo-mass assignment.

6. SUMMARY AND DISCUSSION

In this paper we have used a large galaxy group catalogue constructed from the SDSS Data Release 4 (DR4) to study how the clustering of galaxy groups depends on their masses and, at fixed mass, on the color of their member galaxies. We use the projected and redshift-space two-point cross correlation functions between groups and galaxies to measure the relative biases for groups of different masses and colors. Our main results can be summarized as follows:

1. The correlation amplitude of galaxy groups depends strongly on their masses, and is in good agreement with the mass dependence of the bias of dark matter halos in the ΛCDM concordance cosmology.

2. For a given mass, the correlation amplitude of groups also depends on the characteristic color of its member galaxies. Red groups are more

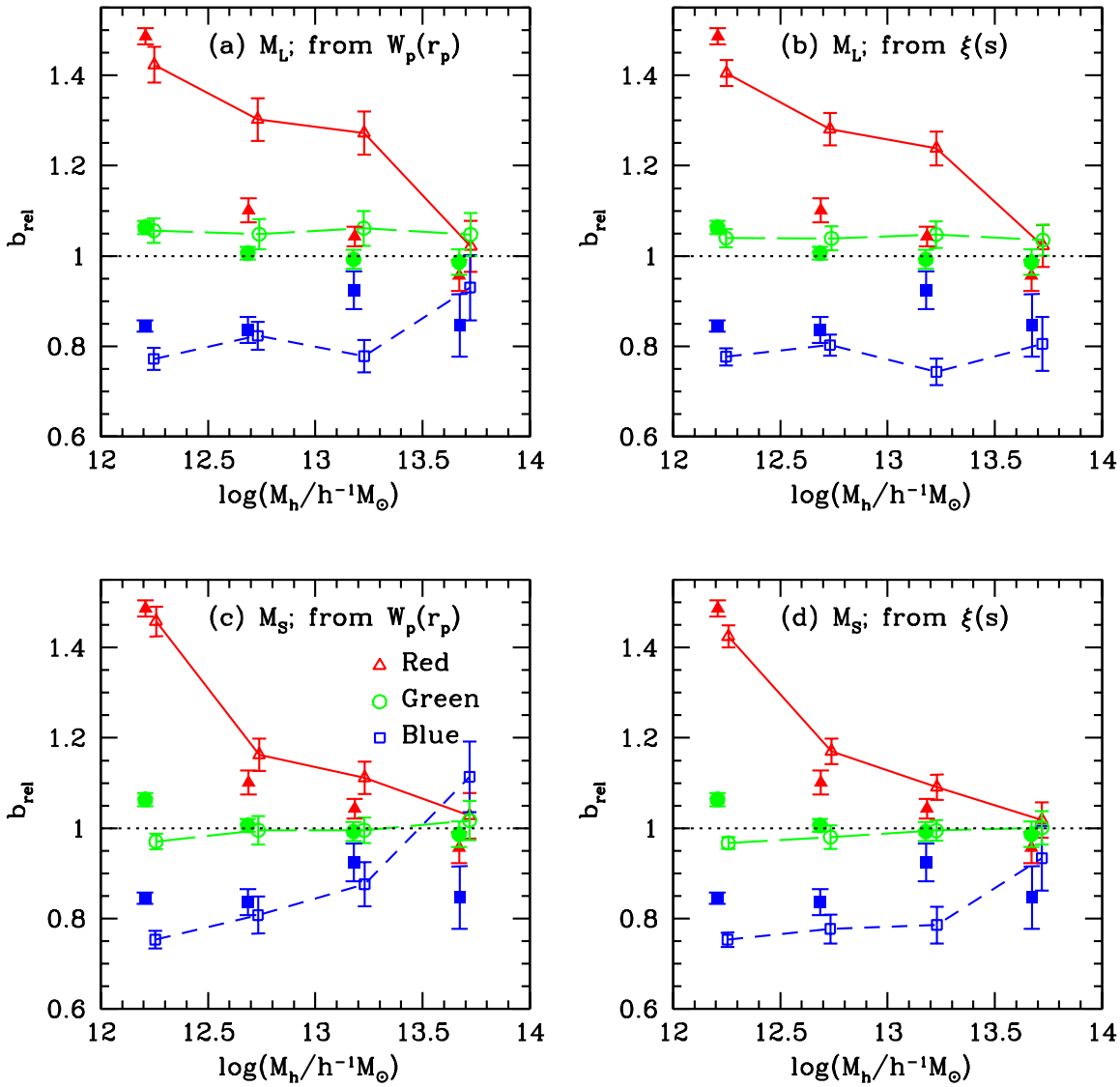

FIG. 13.— Similar to Fig. 8, but for results obtained from the MGRS (open symbols with lines connected). Note that, for comparison, the solid symbols in this plot are results obtained from the *original* Millennium simulation galaxy and halo catalogues, and the real space auto correlation functions are used in measuring the average relative biases. For clarity, the latter set of data are slightly shifted to left hand side.

strongly clustered than blue groups. This color dependence is more prominent in low-mass groups, and becomes insignificant in groups with masses $\gtrsim 10^{14}\ h^{-1}\mathrm{M}_{\odot}$. These results are in good, qualitative agreement with those obtained by Yang et al. (2005b) from an analysis of galaxy groups in the 2dFGRS, but disagree with the results obtained by Berlind et al. (2006a).

3. The observed color dependence in the data is qualitatively reproduced by the semi-analytical model of Croton et al. (2006), but the predicted color dependence is much too strong for low-mass halos with $M \sim 10^{12}h^{-1}\,\mathrm{M}_{\odot}$.

4. The systematic errors that can be induced by the group finder or by the method of assigning masses to the groups are discussed. And we conclude that our finding of the color dependence of the relative bias in the SDSS observation is robust.

Unlike the mass dependence of the group clustering which can be straightforwardly linked to the mass dependence of the halo bias, an interpretation of the color dependence at fixed mass is less straightforward. It is tempting to link it to the assembly bias that has recently been discovered in numerical simulations, and which shows that haloes of a given mass that assemble earlier are more strongly clustered. The assembly time of a dark matter halo, $t_{\rm main}$, is typically defined as the look-back time at which its main progenitor reaches a mass that is half of the halo's present day mass.

A straightforward, but naive, interpretation of our results therefore is that halos that assemble earlier contain redder galaxies. This would not only explain the sign of the color-dependence at fixed halo mass detected here, but since the assembly bias becomes less significant for more massive halos (e.g., Gao et al. 2005; Jing et al. 2007), it also naturally explains why the color-dependence is weaker for more massive groups. One way to invoke a positive, causal correlation between the as-

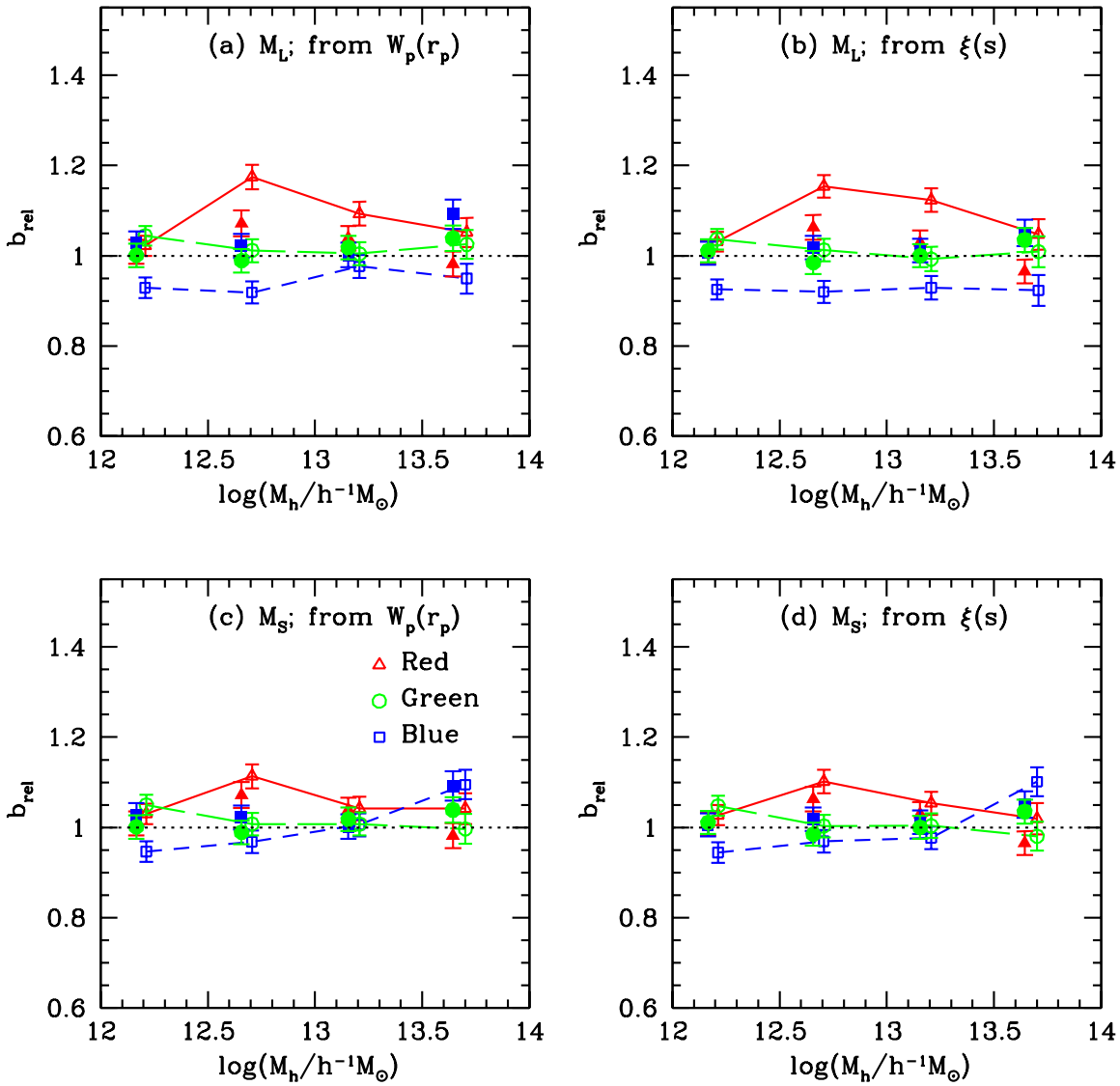

FIG. 14.— Similar to Fig. 13, but for results obtained from the MGRS with randomly re-assigned galaxy colors according to the color-stellar mass distributions of the central and satellite galaxies separately in the SDSS observations. See text for details.

sembly histories of dark matter haloes and the star formation histories of the associated galaxies, is to assume that the epoch of the last major merger, which is strongly correlated with the assembly time (Li et al. 2007b), also signals the time at which star formation is terminated. This may come about if the feedback from merger induced AGN activity expels (or heats) the gas associated with the merger remnant, thus shutting off the star formation activity (e.g., Di Matteo, Springel & Hernquist 2005; Hopkins et al. 2006, 2007). Such a merger induced truncation mechanism would ensure that halos that assemble earlier contain redder galaxies.

Alternatively, the observed color dependence may be related to the 'archeological' downsizing. It is well known that, in hierarchical structure formation, more massive halos assemble later (e.g., Lacey & Cole 1993; van den Bosch 2002; Wechsler et al. 2002). Therefore, if indeed haloes that assemble earlier contain redder galaxies, it would imply that more massive haloes (i.e., clusters) contain bluer galaxies than low mass haloes. This is in clear conflict with observations, which show that more massive galaxies, which typically reside in more massive halos, on average have formed their stars earlier. An attractive solution to this problem has been proposed by Neistein et al. (2006), who introduced an alternative 'halo formation time', the time at which the sum over the masses of *all* the virialized progenitors with masses above a given minimum mass, reaches half the present day halo mass. As shown by Neistein et al. (2006), contrary to the assembly time, $t_{\rm main}$, defined as the accretion time of the last main progenitor, $t_{\rm all}$ *increases* with increasing halo mass, so that it provides a natural explanation for the observed archeological downsizing that galaxies in more massive haloes have older stellar populations. If the star formation history of a galaxy is correlated with this formation time, it may also explain the color-bias at fixed halo mass. The reason is that, as demonstrated in Neistein et al. (2006), although the formation time, $t_{\rm all}$, and the assembly time, $t_{\rm main}$, of halos are anti-correlated when considering the entire halo population, at fixed halo mass $t_{\rm all}$ and $t_{\rm main}$ are positively correlated. Thus, at fixed halo mass, a halo that forms earlier will contain a redder

galaxy and will also assemble earlier.

ACKNOWLEDGMENTS

YW and XY acknowledge the Max-Plank Institute for Astrophysics for hospitality and financial support where this work was finalized. We thank Cheng Li for useful discussions, Liang Gao for providing us the data in electronic form and the anonymous referee for helpful comments that greatly improved the presentation of this paper. XY is supported by the *One Hundred Talents* project, Shanghai Pujiang Program (No. 07pj14102), 973 Program (No. 2007CB815402), the CAS Knowledge Innovation Program (No. KJCX2-YW-T05), and grants from NSFC (Nos. 10533030, 10673023). HJM would like to acknowledge the support of NSF AST-0607535, NASA AISR-126270 and NSF IIS-0611948. The Millennium Run simulation used in this paper was carried out by the Virgo Supercomputing Consortium at the Computing Centre of the Max-Planck Society in Garching. The semi-analytic galaxy catalogue is publicly available at http://www.mpa-garching.mpg.de/galform/agnpaper.

REFERENCES

Adelman-McCarthy J. K., Agüeros M. A., Allam S. S., Anderson K. S. J., Anderson S. F., Annis J., Bahcall N. A., Baldry I. K., et al., 2006, ApJS, 162, 38
Bahcall, N. A., West, M. J., 1992, ApJ, 392, 419
Baldry, I. K., Glazebrook, K., Brinkmann, J., Ivezić, Željko; Lupton, R. H., Nichol, R. C., Szalay, A. S. ,2004 , ApJ, 600 ,681
Baldry, I. K., Balogh, M. L., Bower, R. G., Glazebrook, K., Nichol, R. C., Bamford, S. P., Budavari, T., 2006, MNRAS, 373, 469
Barrow, J. D., Bhavsar, S. P., Sonoda, D. H., 1984, MNRAS, 210, 19
Beers T.C., Flynn K., Gebhardt K., 1990, AJ, 100, 32
Berlind, A. A., & Weinberg, D. H. 2002, ApJ, 575, 587
Berlind A.A., Weinberg D.H., Benson A.J., Baugh C.M., Cole S., Dave R., Frenk C.S., Jenkins A., Katz N., Lacey C.G., 2003, ApJ, 593, 1
Berlind, A. A., Kazin, E., Blanton, M. R., Pueblas, S., Scoccimarro, R., Hogg, D. W., 2006a, astro-ph/0610524
Berlind, A. A. et al. 2006b, ApJS, 167, 1
Blanton M. R., Brinkmann J., Csabai I., Doi M., Eisenstein D., Fukugita M., Gunn J. E., Hogg D. W., et al., 2003a, AJ, 125, 2348
Blanton M. R., Hogg D. W., Bahcall N. A., Brinkmann J., Britton M., Connolly A. J., Csabai I., Fukugita M., et al., 2003b, ApJ, 592, 819
Blanton M.R., Eisenstein D.J., Hogg D.W., Schlegel D.J., Brinkmann J., 2005a, ApJ, 629, 143
Blanton M.R. et al. , 2005b, AJ, 129, 2562
Blanton, M. R., Berlind, A. A., 2007, ApJ, 664, 791
Collister, A. A., & Lahav, O. 2005, MNRAS, 361, 415
Cooray, A., & Sheth, R. 2002, Phys. Rep. 372, 1
Cooray A., 2006, MNRAS, 365, 842
Colless, M., & The 2dFGRS team 2001, MNRAS, 328, 1039
Croton, D. J., S., Volker, White, Simon D. M. , et al., 2006, MNRAS,365 ,11
Croton, D. J., Gao, L., White, S. D. M., 2007, MNRAS, 374, 1303
Davis, M., Peebles, P.J.E. 1983, ApJ 267,465
de Vaucouleurs, G., de Vaucouleurs, A., Corwin, H. G., Buta, R. J., Paturel, G., & Fouque, P. 1991, Third Reference Catalogue of Bright Galaxies (Volume 1-3, XII, 2069 pp. 7 figs.. Springer-Verlag Berlin Heidelberg New York)
Di Matteo T., Springel V., Hernquist L., 2005, Nature, 433, 604
Gao, L., Springel, V., & White, S. D. M. 2005, MNRAS, 363, L66
Gao L., White S. D. M., 2007, MNRAS, 377, L5
Hahn O., Porciani C., Carollo C.M., Dekel A., 2007, MNRAS, 375, 489
Harker, G.; Cole, S.; Helly, J.; Frenk, C.; Jenkins, A. 2006, MNRAS, 367, 1039
Hopkins P.F., Hernquist L., Cox T.J., Di Matteo T., Robertson B., Springel V., 2006, ApJS, 163, 1
Hopkins P.F., Hernquist L., Cox T.J., Keres D., 2007, preprint (arXiv:0706.1243)
Jing, Y. P., Mo, H. J., & Börner, G. 1998, ApJ, 494, 1
Jing, Y. P., Suto, Y., Mo, H. J., 2007 , ApJ, 657, 664
Keselman J.A., Nusser A., 2007, MNRAS, preprint (arXiv:0707.4361)
Lacey C., Cole S., 1993, MNRAS, 262, 627
Li C., Kauffmann G., Jing Y.P., White S.D.M., Börner G., Cheng F.Z., 2006, MNRAS, 368 , 21
Li C., Jing Y.P., Kauffmann G., Börner G., Kang X., Wang L., 2007a, MNRAS, 376 ,984
Li Y., Mo H.J., van den Bosch F.C., Lin W.P., 2007b, MNRAS, 379, 689
Magliocchetti M., Porciani C., 2003, MNRAS, 346, 186
Mo H. J., Jing Y.P., Börner G., 1992, ApJ, 392, 452
Mo H. J., & White S.D.M. 1996, MNRAS, 282, 347
Nagashima, M., Yoshii, Y., 2004, ApJ, 610, 23
Neistein E., van den Bosch F.C., Dekel A., 2006, MNRAS, 372, 933
Padilla N.D., et al., 2004, MNRAS, 352 ,211
Peacock J. A., Smith R. E., 2000, MNRAS, 318, 1144
Press W.H., Schechter P., 1974, ApJ, 187, 425
Reed D.S., Governato F., Quinn T., Stadel J., Lake G., 2007, MNRAS, 378, 777
Saunders W. et al. 2000, MNRAS, 317, 55
Seljak U., 2000, MNRAS, 318, 203
Seljak U., Warren M.S., 2004, MNRAS, 355, 129
Sheth, R.K., Tormen, G., 1999, MNRAS, 308, 119
Sheth, R.K., Mo H.J., Tormen, G., 2001, MNRAS, 323, 1
Sheth, R.K., Tormen, G., 2004, MNRAS, 350, 1385
Springel, V., et al., 2005, Nature, 435, 629
Tinker J.L., Weinberg D.H., Zheng Z., Zehavi I., 2005, ApJ, 631, 41
Tinker, J. L., Conroy, C., Norberg, P., Patiri, S. G., Weinberg, D. H., Warren, M. S., 2007, arXiv0707.3445
Vale A., Ostriker J.P., 2006, MNRAS, 371, 1173
van den Bosch F.C., 2002, MNRAS, 331, 98
van den Bosch F.C., Yang X., Mo H.J., 2003, MNRAS, 340, 771
van den Bosch F.C., Yang X., Mo H.J., Weinmann S.M., Maccio A., More S., Cacciato M., Skibba R., Kang X., 2007, MNRAS, 376, 841
Wang H.Y., Mo H.J., Jing Y.P., 2007, MNRAS, 375, 633
Wechsler R.H., Bullock J.S., Primack J.R., Kravtsov, A. V., Dekel A., 2002 , ApJ, 568, 52
Wechsler R.H., Zentner A.R., Bullock J.S., Kravtsov A.V., Allgood B., 2006 , ApJ, 652 , 71
Weinmann S.M., van den Bosch F.C., Yang X., Mo H.J., 2006a, MNRAS, 366, 2
Weinmann S.M., van den Bosch F.C., Yang X., Mo H.J., Croton D.J., Moore B., 2006b, MNRAS, 372, 1161
Wetzel A.R., Cohn J.D., White M., Holz, D.E., Warren M.S., 2007, ApJ, 656, 139
Yang, X., Mo, H. J., & van den Bosch, F. C. 2003, MNRAS, 339, 1057
Yang, X., Mo, H. J., Jing, Y. P., van den Bosch, F. C., Chu, Y. Q. , 2004 ,MNRAS, 350 , 1153
Yang, X., Mo, H. J., Jing, Y. P., van den Bosch, F. C., Jing, Y. P., 2005a, MNRAS, 356, 1293
Yang, X., Mo, H. J., Jing, Y. P., & van den Bosch, F. C., Jing, Y. P., 2005b, MNRAS, 357, 608
Yang, X., Mo, H. J., & van den Bosch, F. C. 2006, ApJL, 638, 55
Yang, X., Mo, H. J., van den Bosch, F. C., Pasquali, A., Li, C., Barden, M., 2007, ApJ, 671, 153
York, D. G., et al., 2000, AJ, 120, 1579
Zandivarez, A., Merchán, M. E., Padilla, N. D., 2003, MNRAS, 344 ,247
Zheng Z., et al., 2005, ApJ, 633, 791